Opuscula Math. 45, no. 3 (2025), 307–338
https://doi.org/10.7494/OpMath.2025.45.3.307 Opuscula Mathematica

CALCULATION OF EXPLICIT EXPRESSIONS FOR THE HOPF BIFURCATION LIMIT CYCLES IN DELAY-DIFFERENTIAL EQUATIONS

José Enríquez Gabeiras and Juan Francisco Padial Molina

Communicated by J.I. Díaz

Abstract. This paper introduces a methodology to derive explicit power series approximations for the limit cycle periodic solutions of the Hopf bifurcation in autonomous discrete delay differential equations (DDE). The procedure extends the methodology introduced by Casal and Freedman in 1980, by providing a detailed algorithm that iteratively performs systematic calculations up to any desired order of approximation, ensuring a specific error tolerance for any nonlinear DDE presenting a Hopf bifurcation. The methodology is applied to three relevant delay-differential models to illustrate its features: a recently introduced car-following mobility model that explains oscillations in road traffic, a SIR epidemic model for propagation of diseases with temporary immunity, and a simplified macroeconomic system to model business cycles.

Keywords: delay-differential equations, Hopf bifurcation, Poincaré–Lindstedt method, car-following model, SIR epidemic model, macroeconomic model.

Mathematics Subject Classification: 37M20, 37N30, 65D15, 65H17, 65Q20.

1. INTRODUCTION

We consider the autonomous nonlinear delay differential equation for the vector function $\mathbf{x} \in \mathbb{R}^n$, $n \geq 1$:

$$\mathbf{x}'(t) = \mathbf{g}\left(\lambda, \mathbf{x}(t), \mathbf{x}(t-\lambda)\right), \tag{1.1}$$

where $t \in \mathbb{R}^+$, and $\lambda \in \mathbb{R}^+$ is some parameter. We also consider $\mathbf{g} \in C^k(\mathbb{R}^+ \times \mathbb{R}^n \times \mathbb{R}^n; \mathbb{R}^n)$ with $k \geq 3$, and, without loss of generality, the equilibrium point of the system to be $\mathbf{x}(t) = \mathbf{0}$, at which $\mathbf{g}(\lambda, \mathbf{0}, \mathbf{0}) = \mathbf{0}$ for all $\lambda \geq 0$.

This equation is a particular case of the *Retarded Functional Differential Equation* (*RFDE*) class defined in [14], where, in this instance, $\mathbf{g}$ presents a single, constant delay λ. These equations are also known as constant discrete delay equations [24], and will be subsequently referred to as DDE. In [14] conditions for existence, uniqueness, continuity, differentiability and continuation of the equation solutions are provided. The solutions to this type of equations can undergo the Hopf bifurcation phenomenon

when the parameter λ is varied, such that starting from a specific threshold λ_0 the solution changes from a constant equilibrium to a nonzero periodic solution. In this paper we provide a method to systematically derive explicit expressions for the oscillatory solutions of the Hopf bifurcation of equations of type (1.1) up to any desired approximation order, based on the original method introduced in [5].

In order to assess the stability of the system, the linearized approximation of (1.1) is used:

$$\boldsymbol{\eta}'(t) = \mathbf{P}(\lambda)\boldsymbol{\eta}(t) + \mathbf{Q}(\lambda)\boldsymbol{\eta}(t-\lambda), \tag{1.2}$$

where $\mathbf{P}(\lambda) = \mathbb{J}_{\mathbf{u}}\mathbf{g}(\lambda, \mathbf{u}, \mathbf{v}) \,|_{\mathbf{u}=\mathbf{v}=\mathbf{0}}$ and $\mathbf{Q}(\lambda) = \mathbb{J}_{\mathbf{v}}\mathbf{g}(\lambda, \mathbf{u}, \mathbf{v}) \,|_{\mathbf{u}=\mathbf{v}=\mathbf{0}}$, and $\mathbb{J}_*$ is the Jacobian matrix with respect to the vector $*$. Based on [14, 24], the following assumptions are considered:

Assumption 1.1. *The linear system* (1.2) *has a non-constant periodic solution for some* $\lambda = \lambda_0$*, which is determined by a pair of purely imaginary roots* $\{r_0 = j\omega_0, \overline{r}_0 = -j\omega_0\}$*,* $\omega_0 > 0$*, in the characteristic equation of* (1.2)*, while the other roots of the characteristic equation* $r_i \neq r_0, \overline{r_0}$ *satisfy* $r_i \neq mr_0$ *for any integer* m*.*

Assumption 1.2. *By the differentiability of* $\mathbf{g}$ *and the implicit function theorem, there exist a continuously differentiable family of roots* $r(\lambda)$ *for small deviations of* λ *for which* $Re(r'(\lambda)) \neq 0$*, implying that the roots* $r(\lambda)$ *cross the imaginary axis as* λ *varies.*

These assumptions imply that for small deviations of λ_0 there exist non-constant periodic solutions for the nonlinear equation (1.1) with period close to $2\pi/\omega_0$, as stated by the Hopf Bifurcation Theorem (see [14, Ch. 11, Theorem 1.1] or [24, Theorem 6.1]).

Methods to derive numerical solutions for this type of bifurcations have been widely used for a long time. It is well known that regular asymptotic expansions based on a straightforward parameter variation are usually not uniformly valid due to the presence of secular terms in the expansion. To overcome this problem, techniques known as singular perturbation methods have been introduced to find approximate solutions to ODEs bifurcations, among which the most salient are multiple scales, harmonic balance and Poincaré–Lindstedt methods [17, 25]. More recently they have also been adapted to be applied to other type of equations, like DDEs and fractional calculus equations [4, 13, 21, 26, 27]. Due to the complexity of the calculation of the higher order terms in these methods, the majority of applications have been restricted to systems of equations derived from a scalar differential equation (comparatively easier to manipulate), and the validity of the solution has been only limited to small deviations from the limit value of the bifurcation parameter.

The reference [5] established a new framework to generically tackle DDE bifurcations by extending the Poincaré–Lindstedt method for ODEs to any nonlinear autonomous DDE equation that complies with specific solvability conditions. The paper provides an existence theorem for uniformly valid asymptotic series expansions of the solution, alongside a detailed recursive algorithm for the calculation of such expansions. However, no methodical approach to solve the DDE that arise in each iteration step was provided, thus limiting the applicability of the method to lower order systems up to few orders of approximation, where these calculations are manageable. This paper extends that methodology with an algorithm to systematically perform the calculations of these

intermediate DDEs, thus yielding approximate periodic solutions for equations like (1.1) up to any desired expansion order, allowing the calculation of accurate approximations even for delays significantly greater than the bifurcation delay λ_0.

To illustrate the complete procedure enabled by this extended methodology, we present explicit expressions for the approximate periodic solutions for three relevant problems in the area of delayed systems. First, the original analysis of a new car-following model recently introduced in [19] (nDDE model) is expanded by providing explicit expressions for its periodic equilibrium solutions. Secondly, we include results for an epidemic disease transmission model (SIR model), in which temporary immunity induces oscillations and subsequent epidemic waves, and for which an explicit relationship between the immunity period and the frequency and strength of these waves can be derived. Finally, the method is applied to a financial model that combines the interaction between inflation, interest rate and investment level as an explanation of the apparition of macroeconomic cycles.

2. POINCARÉ–LINDSTEDT METHOD APPLIED TO DDES

2.1. SYSTEM OF EQUATIONS TRANSFORMATION

The Poincaré–Lindstedt method for DDEs requires a number of sequential transformations to the original equation so that any DDE problem is expressed in a general standard form. First we transform equations (1.1) and (1.2) by means of a re-scaling of the time variable, $\hat{t} = t\omega_0$, where ω_0 is the fundamental frequency of the Hopf bifurcation (see Assumption 1.1). Thus, we get the $DDE_{\hat{t}}$ form of the problem:

$$\mathbf{x}'(\hat{t}) = \frac{\mathbf{g}(\hat{\lambda}, \mathbf{x}(\hat{t}), \mathbf{x}(\hat{t}-\hat{\lambda}))}{\omega_0} = \mathbf{f}(\hat{\lambda}, \mathbf{x}(\hat{t}), \mathbf{x}(\hat{t}-\hat{\lambda})), \tag{2.1}$$

$$\boldsymbol{\eta}'(\hat{t}) = \mathbf{A}(\hat{\lambda})\boldsymbol{\eta}(\hat{t}) + \mathbf{B}(\hat{\lambda})\boldsymbol{\eta}(\hat{t}-\hat{\lambda}), \tag{2.2}$$

where $\hat{\lambda} = \lambda\omega_0$, with $\mathbf{A}(\hat{\lambda}) = \mathbf{P}(\lambda)/\omega_0$ and $\mathbf{B}(\hat{\lambda}) = \mathbf{Q}(\lambda)/\omega_0$. The particularization of (2.2) for $\hat{\lambda} = \hat{\lambda}_0 = \lambda_0\omega_0$ has periodic solutions with period 2π, among which we will consider a solution $\mathbf{z}_0(\hat{t})$ that verifies

$$\frac{1}{2\pi}\int_0^{2\pi} |\mathbf{z}_0(\hat{t})|^2 d\hat{t} = 1.$$

Additionally, we denote by L the constant coefficient differential delay operator derived from (2.2) for $\hat{\lambda} = \hat{\lambda}_0$, that will be used in the iterative calculations in later steps of the process:

$$L\boldsymbol{\eta} = \boldsymbol{\eta}'(\hat{t}) - \mathbf{A}(\hat{\lambda}_0)\boldsymbol{\eta}(\hat{t}) - \mathbf{B}(\hat{\lambda}_0)\boldsymbol{\eta}(\hat{t}-\hat{\lambda}_0), \tag{2.3}$$

and we denote the null space of the operator L as $N(L) \subset \mathbb{P}^\infty$, ($\mathbb{P}^\infty$ being the subspace of C^∞ of 2π periodic vector functions). In the case of the Hopf bifurcation, the single

pair of eigenvalues assumed in Assumption 1.1 determines a dimension $\dim(N(L)) = 2$, so we will consider a fixed orthonormal basis $\{\mathbf{v}_1(\hat{t}), \mathbf{v}_2(\hat{t})\}$ for the space $N(L)$.

It will also be necessary to consider the formal adjoint operator L^*:

$$L^*\boldsymbol{\eta} = \boldsymbol{\eta}'(\hat{t}) + \mathbf{A}^T(\hat{\lambda}_0)\boldsymbol{\eta}(\hat{t}) + \mathbf{B}^T(\hat{\lambda}_0)\boldsymbol{\eta}(\hat{t} + \hat{\lambda}_0),$$

with $\dim(N(L^*)) = \dim(N(L)) = 2$ and a fixed orthonormal basis of the space $N(L^*)$ $\{\mathbf{w}_1(\hat{t}), \mathbf{w}_2(\hat{t})\}$, $\mathbf{A}^T$ and $\mathbf{B}^T$ being the transposes of $\mathbf{A}$ and $\mathbf{B}$, respectively.

The Poincaré–Lindstedt method for DDEs is based on the search of the periodic solutions of (2.1) by means of an expansion parameter ε, defined as

$$\frac{1}{\hat{T}} \int_{\hat{T}} |\mathbf{x}(\hat{t})|^2 d\hat{t} = \kappa(\varepsilon) \cdot \varepsilon^2, \tag{2.4}$$

where $\mathbf{x}(\hat{t})$ is the periodic solution with period $\hat{T}$ that arise in the Hopf bifurcation for the delay $\hat{\lambda}$, and $\kappa(\varepsilon)$ is a scaling factor that will be determined during the solution construction (see Remark 2.1). In this way, for any $\varepsilon > 0$ we can change the dependent variable $\mathbf{x}(\hat{t}) = \varepsilon \mathbf{z}(\hat{t})$, so that (2.1) and (2.4) are transformed into the DDE_z form of the problem:

$$\mathbf{z}'(\hat{t}) = \begin{cases} \dfrac{\mathbf{f}\left(\hat{\lambda}, \varepsilon\mathbf{z}(\hat{t}), \varepsilon\mathbf{z}(\hat{t} - \hat{\lambda})\right)}{\varepsilon} & \text{for } \varepsilon \neq 0, \\ \mathbf{A}(\hat{\lambda})\mathbf{z}(\hat{t}) + \mathbf{B}(\hat{\lambda})\mathbf{z}(\hat{t} - \hat{\lambda}) & \text{for } \varepsilon = 0, \end{cases}$$

$$\frac{1}{\hat{T}(\varepsilon)} \int_0^{\hat{T}(\varepsilon)} |\mathbf{z}(\hat{t})|^2 d\hat{t} = \kappa(\varepsilon),$$

where the implicit dependence of the period $\hat{T}$ on ε is noted.

Finally, the time variable is again re-scaled as $\tau = (2\pi/\hat{T}(\varepsilon)) \cdot \hat{t}$, so that the solution is periodic 2π in τ for any $\hat{\lambda}(\varepsilon) > \hat{\lambda}_0$, noting now the implicit dependence of $\hat{\lambda}$ on ε. We then define

$$\mathbf{Z}(\tau, \varepsilon) = \mathbf{z}\left(\frac{\hat{T}(\varepsilon)}{2\pi}\tau\right),$$

so $\mathbf{Z}(\tau, \varepsilon) \in \mathbb{P}$ (space of 2π periodic vector functions). Moreover, we get the expression for the DDE_Z form of the problem:

$$\mathbf{Z}'(\tau, \varepsilon) = \begin{cases} \dfrac{\hat{T}(\varepsilon)}{2\pi} \dfrac{\mathbf{f}\left(\hat{\lambda}(\varepsilon), \varepsilon\mathbf{Z}(\tau, \varepsilon), \varepsilon\mathbf{Z}\left(\tau - \frac{2\pi}{\hat{T}(\varepsilon)}\hat{\lambda}(\varepsilon), \varepsilon\right)\right)}{\varepsilon} & \text{for } \varepsilon \neq 0, \\ \mathbf{A}(\hat{\lambda}_0)\mathbf{Z}(\tau, 0) + \mathbf{B}(\hat{\lambda}_0)\mathbf{Z}(\tau - \hat{\lambda}_0, 0) & \text{for } \varepsilon = 0, \end{cases} \tag{2.5}$$

$$\frac{1}{2\pi} \int_0^{2\pi} |\mathbf{Z}(\tau, \varepsilon)|^2 d\tau = \kappa(\varepsilon). \tag{2.6}$$

Notice that for $\varepsilon = 0$ we have $\mathbf{Z}(\tau, 0) = \mathbf{z}_0(\tau)$, and

$$\frac{1}{2\pi}\int_0^{2\pi} |\mathbf{Z}(\tau,0)|^2 d\tau = \frac{1}{2\pi}\int_0^{2\pi} |\mathbf{z}_0(\tau)|^2 d\tau = 1 = \kappa(0).$$

We finally select any linear functional $\Phi : \mathbb{P} \longrightarrow \mathbb{R}$ that verifies

$$\Phi \mathbf{z}_0 = 0,$$

which allows us to define the additional equation

$$\Phi \mathbf{Z} = 0. \tag{2.7}$$

The role of this functional is to set a specific time reference for the solution, given that we will build a periodic solution lacking any particular initial condition. This completes the system of equations (2.5), (2.6) and (2.7), which is verified for $\varepsilon = 0$ by $\mathbf{Z}_0(\tau)$.

2.2. SOLUTIONS AS SERIES EXPANSION

Having set the original equations in terms of the new variables, we express the solutions of $\mathbf{Z}(\tau, \varepsilon)$, $\hat{\lambda}(\varepsilon)$ and $\hat{T}(\varepsilon)$ as asymptotic power series expansions on ε:

$$\begin{aligned} \mathbf{Z}(\tau,\varepsilon) &= \sum_{j=0}^{m} \mathbf{Z}_j(\tau)\varepsilon^j + O(\varepsilon^{m+1}), \\ \hat{\lambda}(\varepsilon) &= \sum_{j=0}^{m} \hat{\lambda}_j \varepsilon^j + O(\varepsilon^{m+1}), \\ \hat{T}(\varepsilon) &= \sum_{j=0}^{m} \hat{T}_j \varepsilon^j + O(\varepsilon^{m+1}), \end{aligned} \tag{2.8}$$

where $\mathbf{Z}_j : \mathbb{R}^+ \to \mathbb{R}^n$ and $\mathbf{Z}_j(\tau) \in \mathbb{P}$. The values $\hat{\lambda}_0 = \lambda_0 \cdot \omega_0$ and $\hat{T}_0 = 2\pi$ are known. In addition, we define the linear functional Φ in (2.7) as the one that zeroes the first component of the solution vector $\mathbf{Z}$ in $\tau = 0$:

$$\Phi \mathbf{Z} = \Phi \mathbf{Z}(\cdot, \varepsilon) = \mathbf{Z}^1(0, \varepsilon) = 0, \tag{2.9}$$

where the superscript $[]^1$ denotes the first component of a vector. The calculation starts by determining $\mathbf{Z}_0(\tau) = \mathbf{z}_0(\tau)$ from the basis $\{\mathbf{v}_1, \mathbf{v}_2\}$ such that it verifies (2.9):

$$\mathbf{Z}_0^1(0) = 0. \tag{2.10}$$

In the following we summarize the methodology of iterative calculations introduced in [5].

2.2.1. Equation for order j of ε

In order to set the notation, we first note the general expression of the Taylor expansion of $\mathbf{f}(\hat{\lambda}, \mathbf{x}, \mathbf{y})$ around the equilibrium point $(\mathbf{x}_0, \mathbf{y}_0) = (\mathbf{0}, \mathbf{0})$ as

$$\mathbf{f}(\hat{\lambda}, \mathbf{x}, \mathbf{y}) = \mathbf{A}(\hat{\lambda})\mathbf{x} + \mathbf{B}(\hat{\lambda})\mathbf{y} + C(\hat{\lambda}, \mathbf{x}, \mathbf{x}) + D(\hat{\lambda}, \mathbf{x}, \mathbf{y}) + E(\hat{\lambda}, \mathbf{y}, \mathbf{y}) + r(\hat{\lambda}, \mathbf{x}, \mathbf{y}), \quad (2.11)$$

with C, D and E representing the quadratic terms of the expansion (bilinear forms), while r represents the remaining higher order terms.

The solution of the system is found by first introducing the series expansion of the variables in (2.8) in the DDE_Z equation (2.5), and equating the terms for the same powers of ε. Then, for $j \geq 1$, we get

$$\mathbf{Z}'_j(\tau) = \varepsilon^j \text{ term of } \mathit{Series}\left(\frac{\hat{T}(\varepsilon)}{2\pi} \frac{\mathbf{f}\left(\hat{\lambda}(\varepsilon), \varepsilon\mathbf{Z}(\tau, \varepsilon), \varepsilon\mathbf{Z}\left(\tau - \frac{2\pi}{\hat{T}(\varepsilon)}\hat{\lambda}(\varepsilon), \varepsilon\right)\right)}{\varepsilon} \right), \quad (2.12)$$

which, inserting in (2.12) the expression of $\mathbf{f}$ in (2.11), can be expressed for any j as the following nonhomogeneous linear DDE, that we will call DDE_{Z_j}:

$$\mathbf{Z}'_j(\tau) = \mathbf{A}(\hat{\lambda}_0)\mathbf{Z}_j(\tau) + \mathbf{B}(\hat{\lambda}_0)\mathbf{Z}_j(\tau - \hat{\lambda}_0) + \mathbf{h}_j(\tau), \quad (2.13)$$

where $\mathbf{h}_j(\tau)$ depends on the terms $\mathbf{Z}_k(\tau), k < j$, and verifies, by (2.3):

$$\mathbf{h}_j(\tau) = L\mathbf{Z}_j.$$

In order to express the structure of $\mathbf{h}_j(\tau)$, we also define the operators $M, N : \mathbf{V} \in \mathbb{R}^n \to \mathbb{R}^n$:

$$M\mathbf{V} = C(\hat{\lambda}_0, \mathbf{Z}_0(\tau), \mathbf{V}) + \frac{D(\hat{\lambda}_0, \mathbf{V}, \mathbf{Z}_0(\tau - \hat{\lambda}_0))}{2}, \quad (2.14)$$

$$N\mathbf{V} = \frac{D(\hat{\lambda}_0, \mathbf{Z}_0(\tau), \mathbf{V})}{2} + E(\hat{\lambda}_0, \mathbf{Z}_0(\tau - \hat{\lambda}_0), \mathbf{V}). \quad (2.15)$$

In terms of the defined notation, the following relationship arises:

$$\begin{aligned} \mathbf{h}_j(\tau) &= L\mathbf{Z}_j(\tau) \\ &= \hat{T}_j\mathbf{R}(\tau) + \hat{\lambda}_j\mathbf{S}(\tau) + M\mathbf{Z}_{j-1}(\tau) + N\mathbf{Z}_{j-1}(\tau - \hat{\lambda}_0) + \mathbf{P}_j(\tau), \end{aligned} \quad (2.16)$$

with

$$\mathbf{R}(\tau) = \frac{1}{2\pi}\left(\mathbf{Z}'_0(\tau) + \hat{\lambda}_0\mathbf{B}(\hat{\lambda}_0)\mathbf{Z}'_0(\tau - \hat{\lambda}_0)\right), \quad (2.17)$$

$$\mathbf{S}(\tau) = \mathbf{A}'(\hat{\lambda}_0)\mathbf{Z}_0(\tau) + \mathbf{B}'(\hat{\lambda}_0)\mathbf{Z}_0(\tau - \hat{\lambda}_0) - \mathbf{B}(\hat{\lambda}_0)\mathbf{Z}'_0(\tau - \hat{\lambda}_0), \quad (2.18)$$

where $\mathbf{A}'(\hat{\lambda}) = \frac{\partial \mathbf{A}(\hat{\lambda})}{\partial \hat{\lambda}}$, $\mathbf{B}'(\hat{\lambda}) = \frac{\partial \mathbf{B}(\hat{\lambda})}{\partial \hat{\lambda}}$, and $\mathbf{P}_j(\tau)$ is a 2π periodic function depending on the following variables:

$$\mathbf{P}_j(\tau) \equiv \mathbf{P}_j(\mathbf{Z}_0(\tau), \ldots, \mathbf{Z}_{j-1}(\tau), \hat{\lambda}_0, \ldots, \hat{\lambda}_{j-1}, \hat{T}_0, \ldots, \hat{T}_{j-1}),$$

with $\mathbf{P}_1 = \mathbf{0}$. So we get from (2.16) a different DDE for each order of ε, which expresses $\mathbf{Z}_j$ in terms of $\hat{\lambda}_k$, $\hat{T}_k$, and $\mathbf{Z}_k(\tau), k = 0, \ldots, j-1$.

To calculate $\mathbf{Z}_j(\tau)$ we use two additional equations. From (2.9)

$$\mathbf{Z}_j^1(0) = 0, \tag{2.19}$$

and, from (2.6), we define a new equation for $\mathbf{Z}_j(\tau)$ by taking an arbitrary real number q_j such that

$$\int_0^{2\pi} \langle \mathbf{Z}_0(\tau), \mathbf{Z}_j(\tau) \rangle \, d\tau = q_j. \tag{2.20}$$

Remark 2.1. The choice of the q_j is not critical for the final solution construction. Choosing different $\{q_j\}$ sets will produce different $\{\mathbf{Z}_j(\tau)\}$, $\{\hat{\lambda}_j\}$ and $\{\hat{T}_j\}$ solution sets, but all of them will eventually converge to the same solution with a different value of ε. This is the reason for introducing the scaling factor $\kappa(\varepsilon)$ in (2.4) in the solution construction: different $\{q_j\}$ sets produce different $\kappa(\varepsilon)$, but the quantity $\kappa(\varepsilon) \cdot \varepsilon^2$ in (2.4) remains constant. Nevertheless, it must also be noted that a sensible choice of the set $\{q_j\}$ will have impact on the speed of the convergence of the series to the final solution. In our numerical experience, assuming the proximity of the final solution to the initial solution $\mathbf{Z}_0(\tau)$, lower values of $\{q_j\}$ produce a quicker convergence, so we use $q_j = 0$ for all j in the included examples.

Now we introduce the conditions for the system solvability.

Definition 2.2. The system (2.5), (2.6) and (2.7) is formally solvable when the following conditions are met:

(i) there exist unique $\hat{\lambda}_1$ and $\hat{T}_1$ such that

$$\int_0^{2\pi} \left\langle \hat{T}_1 \mathbf{R}(\tau) + \hat{\lambda}_1 \mathbf{S}(\tau) + M\mathbf{Z}_0(\tau) + N\mathbf{Z}_0(\tau - \hat{\lambda}_0), \mathbf{w}_i(\tau) \right\rangle d\tau = 0, \quad i = 1, 2,$$

(ii) it is verified that

$$\int_0^{2\pi} \left\langle \hat{T}\mathbf{R}(\tau) + \hat{\lambda}\mathbf{S}(\tau), \mathbf{w}_i(\tau) \right\rangle d\tau = 0, \quad i = 1, 2 \implies \hat{\lambda} = 0, \hat{T} = 0, \tag{2.21}$$

where $\{\mathbf{w}_1(\hat{t}), \mathbf{w}_2(\hat{t})\}$ is the orthonormal basis of the null space of the adjoint operator $N(L^*)$.

Remark 2.3. The two conditions given in Definition 2.2 are sufficient for the system (2.16), (2.19) and (2.20) to have a unique solution $\mathbf{Z}_j(\tau)$ for any q_j and $\mathbf{P}_j$. Indeed, condition (2.21) means that $\text{span}(\{\mathbf{R}(\tau), \mathbf{S}(\tau)\}) \subset N(L^*)$, so, considering the orthogonality condition of $R(L)$ with respect to the null space of the adjoint operator (i.e. $R(L) = N(L^*)^{\perp}$), we have what follows.

For any $\left\{\hat{T}_j, \hat{\lambda}_j\right\} \subset \mathbb{R}$ such that

$$\int_0^{2\pi} \left\langle \hat{T}_j \mathbf{R}(\tau) + \hat{\lambda}_j \mathbf{S}(\tau), \mathbf{w}_i(\tau) \right\rangle d\tau = k_i, \quad i = 1, 2,$$

there exists a unique $\mathbf{Q}_j(\tau) \in N(L^*)$, $\mathbf{Q}_j(\tau) = -\hat{T}_j \mathbf{R}(\tau) - \hat{\lambda}_j \mathbf{S}(\tau)$ such that

$$\int_0^{2\pi} \langle \mathbf{Q}_j, \mathbf{w}_i(\tau) \rangle \, d\tau = -k_i, \quad i = 1, 2.$$

Taking $\mathbf{P}_j(\tau) = \mathbf{Q}_j(\tau) - M\mathbf{Z}_{j-1}(\tau) - N\mathbf{Z}_{j-1}(\tau - \hat{\lambda}_0)$ ensures the verification of the orthogonality condition.

Conversely, for any $\mathbf{P}_j(\tau) \in \mathbb{P}$ such that

$$\int_0^{2\pi} \left\langle \mathbf{P}_j + M\mathbf{Z}_{j-1}(\tau) + N\mathbf{Z}_{j-1}(\tau - \hat{\lambda}_0), \mathbf{w}_i(\tau) \right\rangle d\tau = k_i, \quad i = 1, 2,$$

there exist unique $\left\{\hat{T}_j, \hat{\lambda}_j\right\} \subset \mathbb{R}$ such that

$$\int_0^{2\pi} \left\langle \hat{T}_j \mathbf{R}(\tau) + \hat{\lambda}_j \mathbf{S}(\tau), \mathbf{w}_i(\tau) \right\rangle d\tau = -k_i, \quad i = 1, 2,$$

verifying the orthogonality condition.

This, together with equations (2.19) and (2.20) (for any q_j), ensure the uniqueness of $\mathbf{Z}_j(\tau)$, which hence iteratively determine a unique solution for the system (2.5), (2.6) and (2.7).

To determine $\mathbf{h}_j(\tau)$ in equation (2.13), we first must determine the unknown values for $\hat{\lambda}_j$ and $\hat{T}_j$. Using once again the orthogonality condition $R(L) = N(L^*)^{\perp}$, we get

$$\int_0^{2\pi} \langle L\mathbf{Z}_j(\tau), \mathbf{w}_i(\tau) \rangle \, d\tau = \int_0^{2\pi} \langle \mathbf{h}_j(\tau), \mathbf{w}_i(\tau) \rangle \, d\tau = 0, \quad i = 1, 2. \tag{2.22}$$

The system (2.22) generates two equations with the unknowns $\hat{\lambda}_j$ and $\hat{T}_j$, which provides the desired scalar values.

2.2.2. Asymptotic validity of the solution

The asymptotic validity of the solution calculated with the previous algorithm is ensured by the following theorem, whose proof can be found in the original reference.

Theorem 2.4 (Casal, Freedman [5]). *Under Assumption 1.1 and 1.2, for an ε small enough, a sufficient condition for the system of equations* (2.5), (2.6) *and* (2.7) *to possess a unique and smooth solution* $\big(\hat{\lambda}(\varepsilon), \hat{T}(\varepsilon), \mathbf{Z}(\tau,\varepsilon)\big)$, *with* $\mathbf{Z}(\cdot,\varepsilon)$ *periodic* 2π, $\hat{\lambda}(0) = \hat{\lambda}_0$, $\hat{T}(0) = 2\pi$ *and* $\mathbf{Z}(\tau,0) = \mathbf{z}_0(\tau)$, *is that the system is* formally solvable *in the sense of Definition 2.2. Under these conditions the solution* $\hat{\lambda}(\varepsilon), \hat{T}(\varepsilon), \mathbf{Z}(\tau,\varepsilon)$ *will possess asymptotic expansions of the form* (2.8) *with the latter holding uniformly validly in* τ *with* $\mathbf{Z}_j(\tau)$ 2π*–periodic. In these expressions,* $\big(\hat{\lambda}_j, \hat{T}_j, \mathbf{Z}_j(\tau)\big)$ *are recursively the solutions of* (2.16), (2.19) *and* (2.20), *whose existence is guaranteed by the conditions of formal solvability.*

3. PROCEDURE TO OBTAIN A EXPLICIT SOLUTION OF A DESIRED ORDER

3.1. GENERAL EXPRESSION FOR THE SOLUTION OF ORDER j

Equation DDE_{Z_j} (2.13) is the cornerstone to calculate the complete solution by an iterative process starting from $\mathbf{Z}_0(\tau)$ in (2.8). In the example included in [5] the solution for these equations for orders 1 and 2 are directly presented, and there is not indication on how this is accomplished. Moreover, it is clear that for higher orders the DDE_{Z_j} can become highly complex. This problem is addressed in this section, where we provide a systematic approach to derive the solution up to the desired order of expansion for systems of any differential order, which can be efficiently implemented with standard computer tools.

For each order j, after the calculation of $\hat{T}_j$ and $\hat{\lambda}_j$, and with $\mathbf{Z}_k(\tau)$ known for all $k < j$, we look for solutions of (2.16) that are periodic 2π. Equation (2.13) generates a nonhomogeneous DDE whose homogeneous version is coincident with the particularization of (2.2) for $\hat{\lambda} = \hat{\lambda}_0$, i.e.

$$\begin{aligned} L\mathbf{Z}_j(\tau) = \mathbf{h}_j(\tau) &= \mathbf{Z}_j'(t) - \mathbf{A}(\hat{\lambda}_0)\mathbf{Z}_j(\tau) - \mathbf{B}(\hat{\lambda}_0)\mathbf{Z}_j(\tau - \hat{\lambda}_0) \\ &= \hat{T}_j\mathbf{R}(\tau) + \lambda_j\mathbf{S}(\tau) + M\mathbf{Z}_{j-1}(\tau) + N\mathbf{Z}_{j-1}(\tau - \hat{\lambda}_0) + \mathbf{P}_j(\tau), \end{aligned} \tag{3.1}$$

so the nonhomogeneous term $\mathbf{h}_j(\tau) \in \mathbb{P}$, and is dependent on the following variables:

$$\mathbf{h}_j(\tau) \equiv \mathbf{h}_j(\mathbf{Z}_0(\tau), \ldots, \mathbf{Z}_{j-1}(\tau), \hat{\lambda}_0, \ldots, \hat{\lambda}_j, \hat{T}_0, \ldots, \hat{T}_j). \tag{3.2}$$

To look for the periodic solutions $\mathbf{Z}_j(\tau)$ we rely on the expression of the solution of the general linear DDE initial value problem:

$$\mathbf{u}(t) = \boldsymbol{A}\mathbf{u}(t) + \boldsymbol{B}\mathbf{u}(t-r) + \boldsymbol{\Gamma}(t), \quad t \geq 0, \quad \mathbf{u}_0 = \boldsymbol{\phi},$$

where $\boldsymbol{A}, \boldsymbol{B} \in \mathbb{R}^n \times \mathbb{R}^n$ are constant, $\mathbf{u}_0$ is a continuous function $\boldsymbol{\phi}(t) : [-r, 0) \longrightarrow \mathbb{R}^n$ representing the initial condition, and $\boldsymbol{\Gamma}(t) : \mathbb{R}^+ \to \mathbb{R}^n$ is the nonhomogeneous term. The solution of this linear equation can be expressed in terms of the solution for

the homogeneous problem and a particular solution for the nonhomogeneous problem with null initial condition (see [14] and [24]):

$$\mathbf{u}(t) = \mathbf{u}(t, \boldsymbol{\phi}, \boldsymbol{\Gamma}) = \mathbf{u}(t, \boldsymbol{\phi}, \mathbf{0}) + \mathbf{u}(t, \mathbf{0}, \boldsymbol{\Gamma}).$$

Applying this principle to equation DDE_{Z_j} (2.13), we will calculate the periodic solutions of this equation as:

$$\mathbf{Z}_j(\tau) = \overline{\mathbf{Z}}_j(\tau) + \widehat{\mathbf{Z}}_j(\tau), \tag{3.3}$$

where $\overline{\mathbf{Z}}_j(\tau)$ is the general homogeneous solution and $\widehat{\mathbf{Z}}_j(\tau)$ the particular solution for (2.13).

Regarding $\overline{\mathbf{Z}}_j(\tau)$, it is easily calculated from the basis of 2π periodic vectors $\mathbf{v}_i$ for the null space of the operator L given in (2.3):

$$\overline{\mathbf{Z}}_j(\tau) = \sum_{i=1}^{2} \overline{c}_{ji} \mathbf{v}_i(\tau) = \overline{\mathbf{a}}_j \cos(\tau) + \overline{\mathbf{b}}_j \sin(\tau), \tag{3.4}$$

where $\overline{c}_{ji} \in \mathbb{R}$ and $\overline{\mathbf{a}}_j, \overline{\mathbf{b}}_j \in \mathbb{R}^n$.

The calculation of the particular solution $\widehat{\mathbf{Z}}_j(\tau)$ is more involved. We start by noting the structure of the nonhomogeneous term $\mathbf{h}_j(\tau)$ in (3.2) by the following proposition.

Proposition 3.1. *The function $\mathbf{h}_j(\tau)$ can be expressed as a truncated Fourier series up to the index $j+1$, that is,*

$$\mathbf{h}_j(\tau) = \boldsymbol{\alpha}_{j0} + \sum_{k=1}^{j+1} (\boldsymbol{\alpha}_{jk} \cos(k\tau) + \boldsymbol{\beta}_{jk} \sin(k\tau)), \tag{3.5}$$

where $\boldsymbol{\alpha}_{jk}, \boldsymbol{\beta}_{jk} \in \mathbb{R}^n$.

Proof. A solution $\mathbf{Z}_0(\tau)$ to the homogeneous equation

$$\mathbf{Z}_0'(\tau) = \mathbf{A}(\hat{\lambda}_0)\mathbf{Z}_0(\tau) + \mathbf{B}(\hat{\lambda}_0)\mathbf{Z}_0(\tau - \hat{\lambda}_0)$$

can be built from the base $\mathbf{v}_i(\tau)$:

$$\mathbf{Z}_0(\tau) = \sum_{i=1}^{2} C_{0i} \mathbf{v}_i(\tau), \tag{3.6}$$

with $C_{0i} \in \mathbb{R}$.

From Assumption 1.1, the linear equation (1.2) presents a pair of pure imaginary roots $\pm j\omega_0$, so a basis $\{\widetilde{\mathbf{v}}_i(t)\}$, $i = 1, 2$, for the periodic solutions of equation (1.2) can have the form

$$\widetilde{\mathbf{v}}_i(t) = \boldsymbol{\alpha}_i \cos(\omega_0 t) + \boldsymbol{\beta}_i \sin(\omega_0 t),$$

where $\boldsymbol{\alpha}_i, \boldsymbol{\beta}_i \in \mathbb{R}^n$ can be chosen so that the basis $\{\widetilde{\mathbf{v}}_i(t)\}$ is orthonormal.

Then an orthonormal basis for the solutions of equation (2.2) can have the form

$$\mathbf{v}_i(\hat{t}) = \widetilde{\mathbf{v}}_i\left(\frac{\hat{t}}{\omega_0}\right) = \boldsymbol{\alpha}_i \cos(\hat{t}) + \boldsymbol{\beta}_i \sin(\hat{t}). \tag{3.7}$$

So, (3.6) and (3.7) yield that $\mathbf{Z}_0$ is a first order trigonometric polynomial, that is,

$$\mathbf{Z}_0(\tau) = \sum_{i=1}^{2} C_{0i}\mathbf{v}_i(\tau) = \sum_{i=1}^{2} C_{0i}(\boldsymbol{\alpha}_i \cos(\tau) + \boldsymbol{\beta}_i \sin(\tau)). \tag{3.8}$$

Recalling (3.1), the function $\mathbf{h}_j(\tau)$ has the following form in each step:

$$\mathbf{h}_j(\tau) = \hat{T}_j\mathbf{R}(\tau) + \hat{\lambda}_j\mathbf{S}(\tau) + M\mathbf{Z}_{j-1}(\tau) + N\mathbf{Z}_{j-1}(\tau - \hat{\lambda}_0) + \mathbf{P}_j(\tau). \tag{3.9}$$

We note, for each component of $\mathbf{h}_j(\tau)$ in (3.9), the following properties.

(a) The two first terms are a linear operator on $\mathbf{Z}_0(\tau)$, $\mathbf{Z}_0(\tau - \hat{\lambda}_0)$ and their first derivatives (equations (2.17) and (2.18)), thus yielding a first order trigonometric polynomial.
(b) The third and fourth terms of (3.9) increase the trigonometric order of $\mathbf{Z}_{j-1}(\tau)$ in 1 by means of the bilinear forms M (2.14) and N (2.15) applied to $\mathbf{Z}_{j-1}(\tau)$ and $\mathbf{Z}_{j-1}(\tau - \hat{\lambda}_0)$, respectively.
(c) $\mathbf{P}_j(\tau)$ is a trigonometric polynomial of order $j+1$ by virtue of cross products of $\mathbf{Z}_k$, $k < j$, and their derivatives, plus the expansion term of order j of (2.11).

Finally, taking into account that the order 0 solution $\mathbf{Z}_0(\tau)$ has by (3.8) a trigonometric order 1, the preceding properties (a)–(c) ensure that equation (3.5) is verified for all orders of j, thus proving the proposition. □

The next corollary enable us to calculate $\widehat{\mathbf{Z}}_j(\tau)$.

Corollary 3.2. *The particular solution of* (2.13) $\widehat{\mathbf{Z}}_j(\tau)$ *is a trigonometric polynomial of degree* $j+1$*, which can be expressed as*

$$\widehat{\mathbf{Z}}_j(\tau) = \widehat{\mathbf{a}}_{j0} + \sum_{k=1}^{j+1}(\widehat{\mathbf{a}}_{jk}\cos(k\tau) + \widehat{\mathbf{b}}_{jk}\sin(k\tau)), \tag{3.10}$$

where $\widehat{\mathbf{a}}_{jk}, \widehat{\mathbf{b}}_{jk} \in \mathbb{R}^n$*. Moreover,*

$$\widehat{\mathbf{Z}}'_j(\tau) = \sum_{k=1}^{j+1}(-\widehat{\mathbf{a}}_{jk}k\sin(k\tau) + \widehat{\mathbf{b}}_{jk}k\cos(k\tau)). \tag{3.11}$$

Then the particular solution can be calculated by solving the system obtained by introducing the expressions (3.10) *for* $\mathbf{Z}_j(\tau)$ *and* (3.11) *for* $\mathbf{Z}'_j(\tau)$ *in the identity* DDE_{Z_j} (2.13)*. Equating the coefficients of the same trigonometric term in each of the* n *components produces a linear system of order* $n(2j+3)$ *which provides the desired solution for the coefficients* $\widehat{\mathbf{a}}_{jk}$ *and* $\widehat{\mathbf{b}}_{jk}$*.*

Proof. $\widehat{\mathbf{Z}}_j(\tau)$ and $\widehat{\mathbf{Z}}'_j(\tau)$ must have the same trigonometric degree, so by (2.13) and Proposition 3.1 that degree must be $j+1$. The rest is a consequence of this fact. □

To determine $\mathbf{Z}_j(\tau)$ by (3.3) we need to have $\overline{\mathbf{Z}}_j(\tau)$ and $\widehat{\mathbf{Z}}_j(\tau)$. The particular solution $\widehat{\mathbf{Z}}_j(\tau)$ has been already obtained by Corollary 3.2, so to uniquely determine the solution to the homogeneous equation $\overline{\mathbf{Z}}_j(\tau)$, we get the coefficients $\overline{c}_{ji}$ in (3.4) for every iteration by applying the supplementary conditions for orthogonality and phase with respect to the order 0 solution $\mathbf{Z}_0$.

To get $\mathbf{Z}_j^1(0) = 0$ (see (2.19)), we use the expressions (3.4) and (3.10), such that

$$0 = \mathbf{Z}_j^1(0) = \widehat{\mathbf{Z}}_j^1(0) + \overline{\mathbf{Z}}_j^1(0) = \widehat{\mathbf{a}}_{j0}^1 + \sum_{k=1}^{j+1} \widehat{\mathbf{a}}_{jk}^1 + \overline{c}_{j1}\mathbf{v}_1^1(0) + \overline{c}_{j2}\mathbf{v}_2^1(0). \tag{3.12}$$

From (2.20), we choose $q_j = 0$ for $j \geq 1$:

$$0 = \int_0^{2\pi} \langle \mathbf{Z}_j(\tau), \mathbf{Z}_0(\tau) \rangle \, d\tau = \int_0^{2\pi} \left\langle \widehat{\mathbf{Z}}_j(\tau) + \overline{\mathbf{Z}}_j(\tau), \mathbf{Z}_0(\tau) \right\rangle d\tau. \tag{3.13}$$

The system (3.12)–(3.13) provides the solution for $\overline{c}_{ji}$, $i = 1, 2$, that uniquely determine $\overline{\mathbf{Z}}_j(\tau)$. This finishes the calculation of $\mathbf{Z}_j(\tau)$.

3.2. COMPLETE SOLUTION

Following this procedure, for the final solution $\mathbf{Z}(\tau, \varepsilon)$ two series expansions are carried out simultaneously, one asymptotic in powers of ε, and the other Fourier-type in periods multiple of 2π.

$$\mathbf{Z}(\tau, \varepsilon) = \sum_{j=0}^{N} \mathbf{Z}_j(\tau)\varepsilon^j,$$

$$\mathbf{Z}_j(\tau) = \mathbf{a}_{j0} + \sum_{k=1}^{j+1} (\mathbf{a}_{jk}\cos(k\tau) + \mathbf{b}_{jk}\sin(k\tau)),$$

that, together with (3.3), (3.4) and (3.10) yield:

$$\begin{aligned}
&\mathbf{a}_{j0} = \widehat{\mathbf{a}}_{j0}, && && \text{for } k = 0,\\
&\mathbf{a}_{j1} = \widehat{\mathbf{a}}_{j1} + \overline{\mathbf{a}}_j, && \mathbf{b}_{j1} = \widehat{\mathbf{b}}_{j1} + \overline{\mathbf{b}}_j, && \text{for } k = 1,\\
&\mathbf{a}_{jk} = \widehat{\mathbf{a}}_{jk}, && \mathbf{b}_{jk} = \widehat{\mathbf{b}}_{jk}, && \text{for } k > 1.
\end{aligned}$$

At last, the explicit approximate solution to the original equation up to order N is recovered as

$$\mathbf{x}_N(t) = \tilde{\varepsilon} \left(\mathbf{Z}_0 \left(\frac{2\pi}{\hat{T}(\tilde{\varepsilon})} \omega_0 t \right) + \sum_{j=1}^{N} \mathbf{Z}_j \left(\frac{2\pi}{\hat{T}(\tilde{\varepsilon})} \omega_0 t \right) \tilde{\varepsilon}^j \right),$$

where $\tilde{\varepsilon}$ is the solution to the equation

$$\lambda = \frac{1}{\omega_0} \sum_{j=0}^{N} \hat{\lambda}_j \tilde{\varepsilon}^j.$$

3.3. ERROR ESTIMATION

Strict error bounds for approximate solutions in systems of differential equations are difficult to calculate. For ODEs and PDEs the bounds are usually based on specific characteristics of the differential equation, and no general methodology exist. If we denote the differential problem as $\mathbf{x}' = \mathbf{f}(t, \mathbf{x})$ and $\mathbf{x}_N$ as the approximation of order N, it is usually searched a relationship of the error function calculated in some norm $\|\mathbf{x} - \mathbf{x}_N\|$, with the *residual* function $\mathbf{R}_N$ that measures how well $\mathbf{x}_N$ satisfies the differential equation

$$\mathbf{R}_N(t) = \mathbf{x}'_N(t) - \mathbf{f}(t, \mathbf{x}_N(t)).$$

If the problem is well-posed, then it is considered that the residual represents a good measure of the deviation of the approximation from the real solution (see, for instance, [9]).

In the specific case of RFDEs of discrete type, the difficulty of the problem is compounded by the delay terms. There exist recent works that allow to calculate an error bound for approximate periodic solutions in differential delay equations by the estimation of a set of parameters and the verification of three inequalities [12]. Nevertheless, these calculations require a significant amount of computing effort, that may be beyond the effort to calculate the approximation itself. Therefore, given this difficulty and considering the regularity of the problem we are addressing, we use in this paper for the measure of the relative error the supremum norm of the residual in $[0, \hat{T}_N]$, where $\hat{T}_N$ is the period of the approximate solution, i.e.

$$r_r = \frac{\|\mathbf{R}_N(t)\|_\infty}{\|\mathbf{x}'_N(t)\|_\infty} = \frac{\sup\left\{|\mathbf{x}'_N(t) - \mathbf{f}(t, \mathbf{x}_N(t), \mathbf{x}_N(t-\lambda))| : t \in [0, \hat{T}_N]\right\}}{\sup\left\{|\mathbf{x}'_N(t)| : t \in [0, \hat{T}_N]\right\}}. \tag{3.14}$$

In addition to this measure of residual error, in the examples in next section we will also compare the approximate solutions with numerical integrations obtained with the solver routine for DDEs of Maple 2023 (dsolve). This numerical solution, denoted $\tilde{\mathbf{x}}(t)$, becomes quasi-periodic with a period $\tilde{T}$ after a long enough initial time t_0. In addition to numerically verify quasi-periodicity, the precise value of t_0 is further determined by the conditions $\tilde{\mathbf{x}}^1(t_0) = \mathbf{x}^1_N(0) = 0$ and $\operatorname{sgn}\left(d\tilde{\mathbf{x}}^1/dt(t_0)\right) = \operatorname{sgn}\left(d\mathbf{x}^1_N/dt(0)\right)$. Our estimation for the relative error of the calculated solution $\mathbf{x}_N(t)$ with respect to the numerical solution $\tilde{\mathbf{x}}(t)$ is thus based on this time reference:

$$e_r = \frac{\|\tilde{\mathbf{x}}(t_0 + t) - \mathbf{x}_N(t)\|_\infty}{\|\tilde{\mathbf{x}}(t_0 + t)\|_\infty} = \frac{\sup\left\{|\tilde{\mathbf{x}}(t_0 + t) - \mathbf{x}_N(t)| : t \in [0, \tilde{T}]\right\}}{\sup\left\{|\tilde{\mathbf{x}}(t_0 + t)| : t \in [0, \tilde{T}]\right\}}. \tag{3.15}$$

The advantage of this approach is that in the case that the numerical method is error controlled, in the sense that $\|\mathbf{x}(t_0+t)-\tilde{\mathbf{x}}(t_0+t)\|_\infty \leq \delta$, it provides a hard bound for the absolute error of the calculated approximation $\mathbf{x}_N(t)$, that is,

$$\begin{aligned}\|\mathbf{x}(t_0+t)-\mathbf{x}_N(t)\|_\infty &\leq \|\mathbf{x}(t_0+t)-\tilde{\mathbf{x}}(t_0+t)\|_\infty + \|\tilde{\mathbf{x}}(t_0+t)-\mathbf{x}_N(t)\|_\infty \\ &= \delta + \|\tilde{\mathbf{x}}(t_0+t)-\mathbf{x}_N(t)\|_\infty.\end{aligned}$$

In this way we can determine with the aid of the numerical solution $\tilde{\mathbf{x}}(t)$ the minimum expansion order N that provides a maximum error in a specific scenario.

4. NUMERICAL EXAMPLES

4.1. A CAR FOLLOWING MODEL FOR ROAD TRAFFIC ANALYSIS

Many road traffic studies are focused on the determination of the conditions that generate congestion and traffic jams, for which two different approaches are usually used to perform these analyses: the *microscopic model*, where traffic is seen as individual interacting particles, and the *macroscopic model*, where traffic is seen as a compressible fluid.

A typical micro model is the *follow-the-leader* or *car-following* model, where the driver's actions in a vehicle n are induced by the relative motion of the vehicle $n-1$ ahead. Most important among these models are those that consider the influence of the inter-vehicle distance $(X_{n-1}(t)-X_n(t))$ and the difference between their respective velocities $(X'_{n-1}(t)-X'_n(t))$ [1, 8, 10, 11, 18]. We will focus on a new car-following model (nDDE) recently introduced [19] that present advantages from the point of view of the phenomenological explanation and its applicability to realistic driving scenarios.

This new model represents the situation of two vehicles in a single lane (denoted as 0 for the leading car and 1 for the following car). It considers that the leading car has a constant velocity $X'_0(t)=v_0$, and the following variables for the distance between the cars $(s(t))$ and the relative velocity $(s'(t))$:

$$s(t)=(X_0(t)-X_1(t)), \quad s'(t)=(v_0-X'_1(t)).$$

We then have $s''(t)=-X''_1(t)$. The authors in [19] express the retarded dependence of the acceleration as a function of $s(t)$ and $s'(t)$. In this way we have the system (nDDE):

$$-s''(t+\lambda)=X''_1(t+\lambda)=g(s(t),s'(t)), \tag{4.1}$$

where g is the following sigmoid function:

$$g(s,s')=a-\frac{(a+b)}{1+\frac{b}{a}e^{d(s-M+Ks')}}, \quad \forall (s,s')\in\mathbb{R}^2. \tag{4.2}$$

In (4.1) and (4.2) λ is the delay or reaction time, M is the equilibrium distance, d is a parameter to model the intensity of the response of the car-driver ensemble, and K is a parameter to model the driver's response according to the safe distance and the perceived relative velocity.

Reference [19] provides an analysis of the dynamical characteristics of the Hopf bifurcation, showing the change from stability to oscillatory solutions in equilibrium depending on the value of the delay term. It also characterizes the nDDE equation as a Retarded Functional Differential Equation (RFDE) [14], and studies the structure of the solutions produced by this bifurcation and its impact on the traffic process. As an application of the methodology introduced in this paper, next we use it to calculate the explicit expression for the periodic solutions arising near the bifurcation point for this model.

4.1.1. System of equations and equilibrium solution

We start by redefining the variables so that the equilibrium point is $\mathbf{0}$, defining $x_1 = s - M$ and $x_2 = s'$, and transforming equation (4.1) into a system of first order DDEs:

$$\begin{aligned} x_1'(t) &= x_2(t), \\ x_2'(t) &= -a + \frac{(a+b)}{1 + \frac{b}{a} e^{d(x_1(t-\lambda) + K x_2(t-\lambda))}}. \end{aligned} \tag{4.3}$$

Next, we consider the linearized system:

$$\begin{aligned} x_1'(t) &= x_2(t), \\ x_2'(t) &= -D\left(x_1(t-\lambda) + K x_2(t-\lambda)\right), \end{aligned} \tag{4.4}$$

where $D = d\frac{ab}{a+b}$. This system is characterized by the following matrices (as in equation (1.2)):

$$\mathbf{P} = \begin{pmatrix} 0 & 1 \\ 0 & 0 \end{pmatrix}, \quad \mathbf{Q} = \begin{pmatrix} 0 & 0 \\ -D & -DK \end{pmatrix}.$$

In order to calculate the critical delay λ_0 that produces the periodic solution of period ω_0 corresponding to the Hopf bifurcation, we introduce an exponential function as the eigenfunction of the system. Introducing a general solution of the form $\boldsymbol{\alpha} e^{j\omega_0 t}$, with $\boldsymbol{\alpha} \in \mathbb{R}^2$ constant, we get the characteristic equation:

$$\omega_0^2 = D(1 + jK\omega_0) e^{j\omega_0 \lambda_0},$$

which, in turn, generates the following equations corresponding to the real and imaginary parts:

$$K = \frac{\tan(\omega_0 \lambda_0)}{\omega_0}, \qquad D = \omega_0^2 \cos(\omega_0 \lambda_0). \tag{4.5}$$

These two transcendental equations define the bifurcation point (ω_0, λ_0).

We get the following solution basis in terms of the scaled time $\hat{t} = \omega_0 t$:

$$\begin{aligned} \mathbf{v}_1(\hat{t}) &= \frac{1}{\sqrt{\pi(1+\omega_0^2)}} (\cos(\hat{t}), -\omega_0 \sin(\hat{t})), \\ \mathbf{v}_2(\hat{t}) &= \frac{1}{\sqrt{\pi(1+\omega_0^2)}} (\sin(\hat{t}), \omega_0 \cos(\hat{t})). \end{aligned}$$

For the adjoint system, we get the following basis in $\hat{t}$:

$$\mathbf{w}_1(\hat{t}) = \frac{\cos(\omega_0\lambda_0)}{\sqrt{\pi(1+\omega_0^2\cos^2(\omega_0\lambda_0))}}(\omega_0\cos(\hat{t}), \tan(\omega_0\lambda_0)\cos(\hat{t}) - \sin(\hat{t})),$$
$$\mathbf{w}_2(\hat{t}) = \frac{\cos(\omega_0\lambda_0)}{\sqrt{\pi(1+\omega_0^2\cos^2(\omega_0\lambda_0))}}(\omega_0\sin(\hat{t}), \cos(\hat{t}) + \tan(\omega_0\lambda_0)\sin(\hat{t})).$$

4.1.2. Explicit expression of periodic solutions

We will focus on the particular case of system (4.3) with the physical parameters summarized in Table 1.

Table 1
nDDE parameters for the evaluated scenario [19]

Parameter	Description	Value
a	Maximum acceleration in nDDE	2.0576 m/s^2
b	Maximum deceleration	1.5677 m/s^2
v_0	Leader velocity	22.2222 m/s
M	Safe distance for v_0	44.4444 m
d	Car + driver response intensity	0.1124
K	Driver sensitivity to s'	11.3890 s

Under these conditions, the bifurcation point can be calculated from (4.5):

$$\omega_0 = 1.1424,$$
$$\lambda_0 = 1.3079,$$

obtaining the following orthonormal base for the solutions of the linearized system (4.4):

$$\mathbf{v}_1(\hat{t}) = (0.3716\cos(\hat{t}), -0.4245\sin(\hat{t})),$$
$$\mathbf{v}_2(\hat{t}) = (0.3716\sin(\hat{t}), 0.4245\cos(\hat{t})),$$

and the base for the adjoint system:

$$\mathbf{w}_1(\hat{t}) = (0.0492\cos(\hat{t}), -0.0431\sin(\hat{t}) + 0.5604\cos(\hat{t})),$$
$$\mathbf{w}_2(\hat{t}) = (0.0492\sin(\hat{t}), 0.0431\cos(\hat{t}) + 0.5604\sin(\hat{t})).$$

We then use these values to derive the approximations to the solutions of $\mathbf{Z}(\tau,\varepsilon)$, $\hat{\lambda}(\varepsilon)$ and $\hat{T}(\varepsilon)$ by iteratively calculating the terms $\mathbf{Z}_j(\tau)$, $\hat{\lambda}_j$ and $\hat{T}_j$ as described in Sections 2 and 3. We have performed the automation of the symbolic and numerical calculations by means of a program developed on the Maple 2023 platform.

First, using the basis of the linear system $\{\mathbf{v}_1, \mathbf{v}_2\}$, we start by selecting the fundamental solution $\mathbf{Z}_0(\tau)$ so that it is compatible with the phase condition (2.10). This leads us to the choice $\mathbf{Z}_0(\tau) = \sqrt{2\pi}\cdot\mathbf{v}_2(\tau)$. Using this as our first solution, we iteratively calculate the subsequent orders following the described methodology.

The coefficients of the expansions for the vector solution, up to order 5, are included in Tables 2 and 3 (in terms of scaled time $\hat{t} = \omega_0 t$), while Table 4 contains the coefficients for the series expansion of $\hat{\lambda}$ and $\hat{T}$ (in terms of scaled time $\tau = (2\pi/\hat{T}(\varepsilon)) \cdot \hat{t} = (2\pi/\hat{T}(\varepsilon)) \cdot \omega_0 t$). It is worth noting that even when we get null values for the parameters $\hat{\lambda}_i$ and $\hat{T}_i$, as is the case for order 1 and 3, there are still nonzero terms for those orders in the series expansion of the solution.

Table 2
Coefficients for space x_1

Trig. order	$o0$	$o1$	$o2$	$o3$	$o4$	$o5$
Const	0.0	$-5.6e-01$	0.0	$-1.6e-01$	$-4.2e-03$	$-5.6e-02$
$\cos(\tau)$	$9.3e-01$	0.0	$6.3e-02$	0.0	$1.2e-02$	$4.7e-04$
$\sin(\tau)$	0.0	$5.7e-01$	$5.8e-03$	$1.6e-01$	$5.5e-03$	$5.4e-02$
$\cos(2\tau)$		$-4.7e-03$	$1.1e-02$	$1.9e-03$	$3.7e-03$	$9.2e-04$
$\sin(2\tau)$		$-8.9e-03$	$-5.7e-03$	$2.2e-03$	$-1.1e-03$	$1.6e-03$
$\cos(3\tau)$			$2.9e-03$	$6.8e-06$	$-3.7e-03$	$-1.3e-04$
$\sin(3\tau)$			$-3.7e-06$	$5.4e-03$	$9.1e-05$	$-3.0e-04$
$\cos(4\tau)$				$-1.0e-04$	$3.0e-04$	$2.5e-04$
$\sin(4\tau)$				$-1.2e-04$	$-2.6e-04$	$2.7e-04$
$\cos(5\tau)$					$3.1e-05$	$-2.9e-06$
$\sin(5\tau)$					$9.6e-07$	$9.4e-05$
$\cos(6\tau)$						$-2.3e-06$
$\sin(6\tau)$						$-2.3e-06$

Table 3
Coefficients for relative velocity x_2

Trig. order	$o0$	$o1$	$o2$	$o3$	$o4$	$o5$
Const	0.0	0.0	0.0	0.0	0.0	0.0
$\cos(\tau)$	0.0	$-6.5e-01$	$-6.6e-03$	$-1.0e-01$	$-5.5e-03$	$-3.1e-02$
$\sin(\tau)$	1.1	0.0	$-5.5e-02$	0.0	$-1.1e-02$	$-4.1e-04$
$\cos(2\tau)$		$2.0e-02$	$1.3e-02$	$-7.4e-03$	$9.5e-04$	$-3.3e-03$
$\sin(2\tau)$		$-1.1e-02$	$2.5e-02$	$5.6e-03$	$5.4e-03$	$1.7e-03$
$\cos(3\tau)$			$1.3e-05$	$-1.8e-02$	$-3.1e-04$	$3.2e-03$
$\sin(3\tau)$			$1.0e-02$	$2.3e-05$	$-1.4e-02$	$-4.3e-04$
$\cos(4\tau)$				$5.5e-04$	$1.2e-03$	$-1.3e-03$
$\sin(4\tau)$				$-4.8e-04$	$1.4e-03$	$1.2e-03$
$\cos(5\tau)$					$-5.5e-06$	$-5.4e-04$
$\sin(5\tau)$					$1.8e-04$	$-1.7e-05$
$\cos(6\tau)$						$1.5e-05$
$\sin(6\tau)$						$-1.6e-05$

Table 4
Coefficients for series expansion of $\hat{\lambda}$ and $\hat{T}$

Coefficient	o0	o1	o2	o3	o4	o5
$\hat{\lambda}_j$	1.4940	0.0000	0.1666	0.0000	0.0387	0.0013
$\hat{T}_j$	2π	0.0000	0.7465	0.0000	0.1814	0.0056

At this point we are already able to draw the bifurcation diagram for the different components of the solution by representing the maximum and minimum of the oscillations for each value of the delay. This is shown in Figure 1 below. Notice that this diagram is generated almost instantly from the series expansion obtained, with no need to perform numerical integrations for each value of λ, as is customary when no explicit expression for the solution exists.

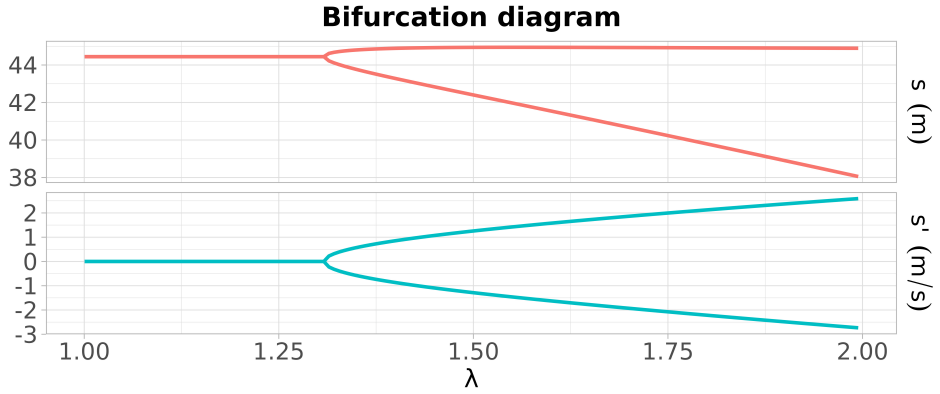

Fig. 1. Bifurcation diagram of s and s' in the nDDE model (4.2)

More detailed results for specific values of delay follow. Given that the periodic solution for values of delay that are very close to the bifurcation value $\lambda_0 = 1.3079$ have very small amplitude, we test delay values sensibly greater to get oscillations with significant amplitudes. The results compare the approximation obtained with the Poincaré–Lindstedt method up to order 8 (referred to as *P-L* or $\mathbf{x}_8$ in the graphs) to the solution calculated by the numerical integration (referred to as *Num*). The Maple routine used is dsolve, using the fourth-fifth order Runge–Kutta method (rkf45) with parameters abserr = relerr = 10^{-9}. The numerical integration results are calculated with an initial condition $x_1(0) = 20\ \ m$ and $x_2(0) = 17.22\ \ m/s$, taking the steady state after a sufficiently large initial time $t_0 > 1000s$, while the explicit calculation by Poincaré–Lindstedt method is directly calculated up to the order 8.

Figure 2(a) presents the comparison of the solutions of system (4.3) for a delay $\lambda = 1.6s$. Note that in the numerical solution graph the time value is relative to t_0. As expected, the closeness of both calculations is remarkable. Figure 2(b) shows the approximate solutions for each series expansion order. In this case, the order expansions beyond order 4 have a marginal contribution to the final approximation.

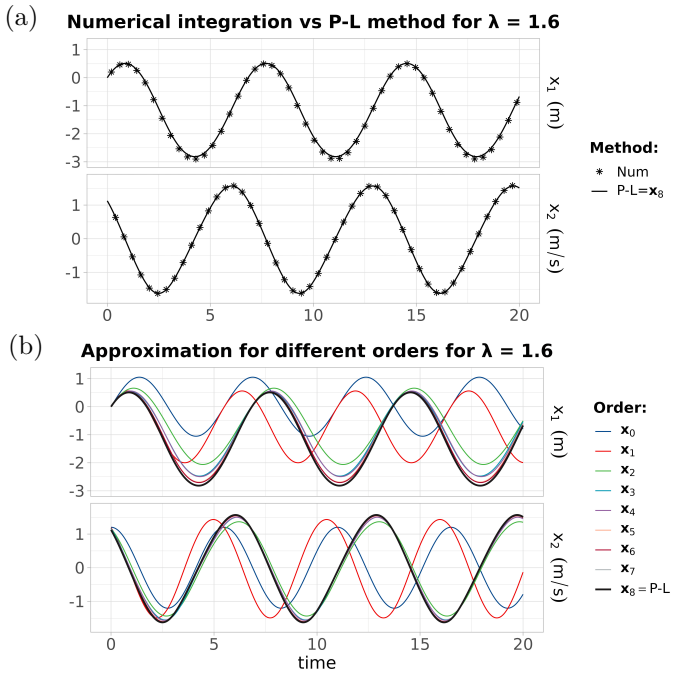

Fig. 2. Asymptotic stable solution of $x_1(t)$ and $x_2(t)$ for $\lambda = 1.6s$ in nDDE (4.3): (a) numerical solution $\tilde{\mathbf{x}}(t_0 + t)$ and P-L calculation $\mathbf{x}_8(t)$, (b) approximation for each series expansion order. $\tilde{\varepsilon} = 1.1303$

4.1.3. Error estimation

Table 5 contains the values for the residual r_r and the relative error e_r from equations (3.14) and (3.15), for three values of delay.

Table 5
Relative errors for the different values of λ

	Error [%]	$\mathbf{x}_2$	$\mathbf{x}_3$	$\mathbf{x}_4$	$\mathbf{x}_5$	$\mathbf{x}_6$	$\mathbf{x}_7$	$\mathbf{x}_8$
$\lambda = 1.4s$	r_r	5.35	4.10	0.71	0.50	0.15	0.09	0.03
	e_r	6.84	11.30	1.27	1.66	0.28	0.33	0.07
$\lambda = 1.6s$	r_r	22.29	29.03	6.68	8.84	3.05	3.93	1.57
	e_r	17.30	42.04	6.35	11.32	2.76	4.49	1.37
$\lambda = 1.8s$	r_r	35.90	51.42	15.52	22.20	8.68	7.75	7.42
	e_r	22.38	74.05	9.50	23.51	4.96	11.43	3.56

The values confirm that the residual r_r is a good indicator of the level of error committed in the calculated solution $\mathbf{x}_N(t)$. Also, these values clearly show how more orders of integration are needed when the value of the delay becomes higher. In any case, calculations up to order 20 have been performed that produce relative errors below 1% for the highest delay $\lambda = 1.8s$.

4.2. SIR EPIDEMIC MODEL

Models for infectious diseases are frequently based on the so-called compartmental models, where the population is divided in separated groups according to the situation with respect to the disease, typically in groups like Susceptible (S), Infected (I), Exposed (E), Recovered (R) and Asymptomatic (A). The flow of population from one group to the other groups are modeled by a set of nonlinear differential equations that take into account the disease characteristics and the possible actions, like vaccination campaigns (see, for instance, [3, 7, 15]). Specially relevant are the models with temporary immunity, in which some time after the recovery (typically some months after the natural infection or the vaccination), a recovered person in group R loses immunity and returns to the susceptible group S. Some studies in this line, using the DDE and Hopf bifurcation framework have been recently published ([2, 16, 20, 22, 23]). We provide in the following section an example of application of the method to explicitly calculate the Hopf bifurcation solutions to a SIR model with temporary immunity.

4.2.1. System of equations and equilibrium solution

We base the analysis on a model proposed in [3, Ch. 10] that considers three population groups: Susceptible (S), Infected (I) and Recovered (R) (the SIR model), and a total population $P = I + S + R$. The model includes births and deaths (both related and not related to the disease), and therefore have a total population P that is variable, which makes the model somewhat more complicated. Thus, the system we will consider is the following:

$$\begin{aligned} I'(t) &= \beta S(t)I(t) - \mu I(t) - \alpha I(t), \\ S'(t) &= \Lambda(P) - \beta S(t)I(t) - \mu S(t) + f\alpha(1-\mu\lambda)I(t-\lambda), \\ R'(t) &= -\mu R(t) + f\alpha I(t) - f\alpha(1-\mu\lambda)I(t-\lambda), \end{aligned} \tag{4.6}$$

where:

- β is the contagion rate, proportional to the product of the susceptible and the infected;
- α is the output rate from the infected state, considering both the deaths and the recovered from the disease;
- f is the fraction of α that recovers, passing from the group I to the group R;
- λ is the immunity period, after which the recovered pass to be susceptible again, passing from the R group to the S group;
- $\Lambda(P)$ is the birth rate and μ is the natural death rate (not related to the disease); the conditions $\lambda(P_{\max}) = \mu P_{\max}$ and $\Lambda'(P_{\max}) < \mu$, where $P_{\max}$ is the maximum population achievable, are necessary to ensure the asymptotic stability (see [3]), so the function that we will use is the following:

$$\Lambda(P) = \Lambda(I+S+R) = \frac{\mu(1+P_{max})P}{1+P}.$$

To evaluate the possible equilibria of the system, it is usually calculated the *basic reproduction number* r_0, defined as the *expected number of secondary cases produced, in a completely susceptible population, by a typical infective individual* [6]. In the case that $r_0 < 1$ then the only asymptotically stable solution is the *disease-free equilibrium* (DFE) ($I_\infty = 0, S_\infty > 0, R_\infty = 0$), i.e., all the population is susceptible and there is no disease because there are not infected individuals. If, on the other hand, $r_0 \geq 1$ then there exists a state called the *endemic equilibrium* (EE), with ($I_\infty > 0, S_\infty > 0, R_\infty > 0$). Reference [7] provides the method to calculate this number for a general compartmental model based on the so called *next generation matrix*, that we have used to calculate:

$$r_0 = \frac{\beta P_{max}}{\mu + \alpha}. \tag{4.7}$$

To calculate the equilibrium points, we solve the steady state equations for (4.6):

$$\begin{aligned} &\beta S_\infty I_\infty - (\mu + \alpha) I_\infty = 0, \\ &\Lambda(I_\infty + S_\infty + R_\infty) - \beta S_\infty I_\infty - \mu S_\infty + f\alpha(1 - \mu\lambda) I_\infty = 0, \\ &-\mu R_\infty + f\alpha\mu\lambda I_\infty = 0. \end{aligned} \tag{4.8}$$

Note that the endemic equilibrium solution $(I_\infty, S_\infty, R_\infty)$ in (4.8) is dependent on λ. Given that the equilibrium solution must be subtracted from the original variables (I, S, R) so that to transform the system (4.6) into a system with equilibrium $\mathbf{0}$, this considerably complicates the expressions of the matrices $\mathbf{P}(\lambda)$ and $\mathbf{Q}(\lambda)$ in (1.2), and therefore the calculation of the bifurcation point (λ_0, ω_0), so computer calculus tools are necessary to derive these expressions.

4.2.2. Explicit expression of periodic solutions

We will study an scenario based on the values of Table 6.

Table 6
Parameters used in the study of the SIR model (4.6)

Parameter	Description	Value
α	Output rate of infected state	0.1 (/infected/day)
β	Contagion rate	0.01 (/infected/susceptible)
μ	Death rate	10^{-4} (/pop/day)
f	Fraction of recovered	0.98
$P_{\max}$	Maximum population	30 ($\times 10^6$)

Using these values we first check the value of the basic reproduction number using (4.7) to get $r_0 = 2.997 > 1$. The endemic equilibrium in this system for these values is calculated using equations (4.8):

$$I_\infty = \frac{1.8 \cdot 10^4\lambda - 3.8 \cdot 10^6 + 3.6 \cdot 10^2\sqrt{2.2 \cdot 10^2\lambda^2 + 3.3 \cdot 10^6\lambda + 1.5 \cdot 10^8}}{3.4 \cdot 10^2\lambda^2 + 7.7 \cdot 10^4\lambda + 7.5 \cdot 10^5},$$
$$R_\infty = 0.098\lambda \cdot I_\infty,$$
$$S_\infty = 10.01.$$

Taking this equilibrium point we calculate $\mathbf{P}(\lambda)$, $\mathbf{Q}(\lambda)$ and the characteristic equation, whose expressions are highly nontrivial and therefore are omitted here. Under these conditions, the bifurcation point is numerically calculated, yielding:

$$\omega_0 = 0.03440,$$
$$\lambda_0 = 102.0308.$$

Considering these values, we obtain the following orthonormal basis for the solutions of the linearized system in the scaled time $\hat{t} = \omega_0 t$:

$$\mathbf{v}_1(\hat{t}) = (0.0712\cos(\hat{t}), -0.3946\sin(\hat{t}), -0.0712\cos(\hat{t}) + 0.3905\sin(\hat{t})),$$
$$\mathbf{v}_2(\hat{t}) = (0.0712\sin(\hat{t}), 0.3946\cos(\hat{t}), -0.0172\sin(\hat{t}) - 0.3905\cos(\hat{t})),$$

and the basis for the adjoint system:

$$\mathbf{w}_1(\hat{t}) = (-0.5555\sin(\hat{t}), -0.0970\cos(\hat{t}) - 0.0178\sin(\hat{t}), -5.1 \cdot 10^{-6}\cos(\hat{t}) + 2.7 \cdot 10^{-5}\sin(\hat{t})),$$
$$\mathbf{w}_2(\hat{t}) = (0.5555\cos(\hat{t}), -0.0970\sin(\hat{t}) + 0.0178\cos(\hat{t}), -5.1 \cdot 10^{-6}\sin(\hat{t}) - 2.7 \cdot 10^{-5}\cos(\hat{t})).$$

We now use these bases to derive the approximations to the solutions of $\mathbf{Z}(\tau, \varepsilon)$, $\hat{\lambda}(\varepsilon)$ and $\hat{T}(\varepsilon)$ using the script developed. Again, we choose as the fundamental solution $\mathbf{Z}_0(\tau) = \sqrt{2\pi} \cdot \mathbf{v}_2(\tau)$ so that it is compatible with the phase condition (2.10). Using this as our first solution, we iteratively calculate the subsequent orders following the described methodology. For the sake of brevity, in this instance we omit the coefficients for the vector solution and just provide the coefficients for the series expansion of $\hat{\lambda}$ and $\hat{T}$ (in terms of the scaled time $\hat{t} = \omega_0 t$) in Table 7.

Table 7
Coefficients for series expansion of λ and $\hat{T}$

Coefficient	o0	o1	o2	o3	o4	o5
$\hat{\lambda}_i$	3.510	0	0.0239	0	$3.3 \cdot 10^{-4}$	$-4 \cdot 10^{-6}$
$\hat{T}_i$	2π	0	0.0398	0	$5.1 \cdot 10^{-4}$	$-6 \cdot 10^{-6}$

Figure 3 shows the bifurcation diagram in this model. Note the non-constant endemic equilibrium solution for delays smaller than the bifurcation value $\lambda_0 = 102.03$ days. Computations for these graphs with a resolution of 200 points took less than 30 seconds with a solution expansion of order 14 using the Maple 2023 platform.

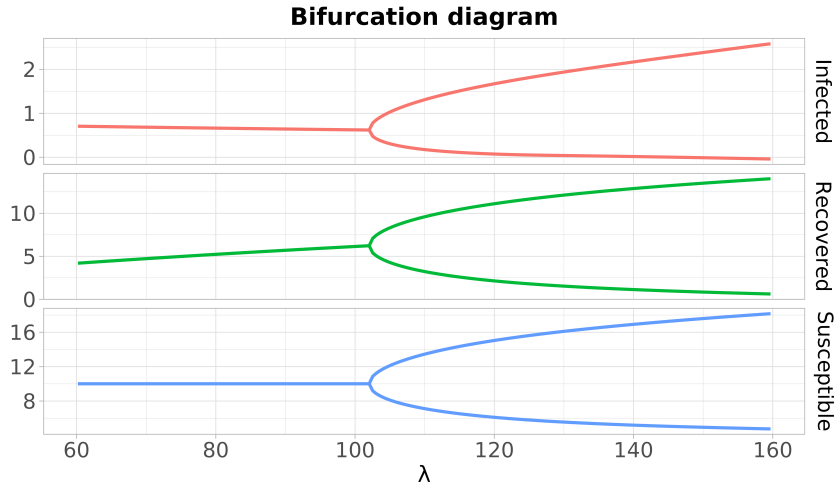

Fig. 3. Bifurcation diagram of I, R and S in the SIR model (4.6)

The results for the approximation obtained with the Poincaré–Lindstedt method compared to the solution calculated by numerical integration are presented next. The numerical integration results are calculated with the initial condition of $I_0 - I_\infty = 10^{-5}$, $S_0 - S_\infty = -10^{-5}$ and $R_0 - R_\infty = 0$, taking the steady state after a sufficiently large initial time, while the explicit calculation by Poincaré–Lindstedt method is directly calculated up to the order 8.

Figure 4 presents the comparison of the solutions of system (4.6) for a delay $\lambda = 140$ days, greater than the Hopf bifurcation threshold $\lambda_0 = 102.03$ days. The solutions in the graphs represent the deviation with respect to the endemic equilibrium point ($I_\infty = 0.5581,\ S_\infty = 10.01,\ R_\infty = 7.6573$). Figure 4 (b) shows the approximate solution up to a certain series expansion order. In this case, the order expansions beyond order 4 have a marginal contribution to the final approximation.

Table 8 show the residual r_r and the relative error with respect to the numerical solution e_r for delay $\lambda = 120$ days and $\lambda = 140$ days. In this instance, calculations up to order 8 ensure a relative error below 1% for the lower delay $\lambda = 120$ days, and comparable error measures using the residual instead of the approximate solution error. To get relative errors below 1% in the case $\lambda = 140$ days we need to calculate at least the expansions up to order 12.

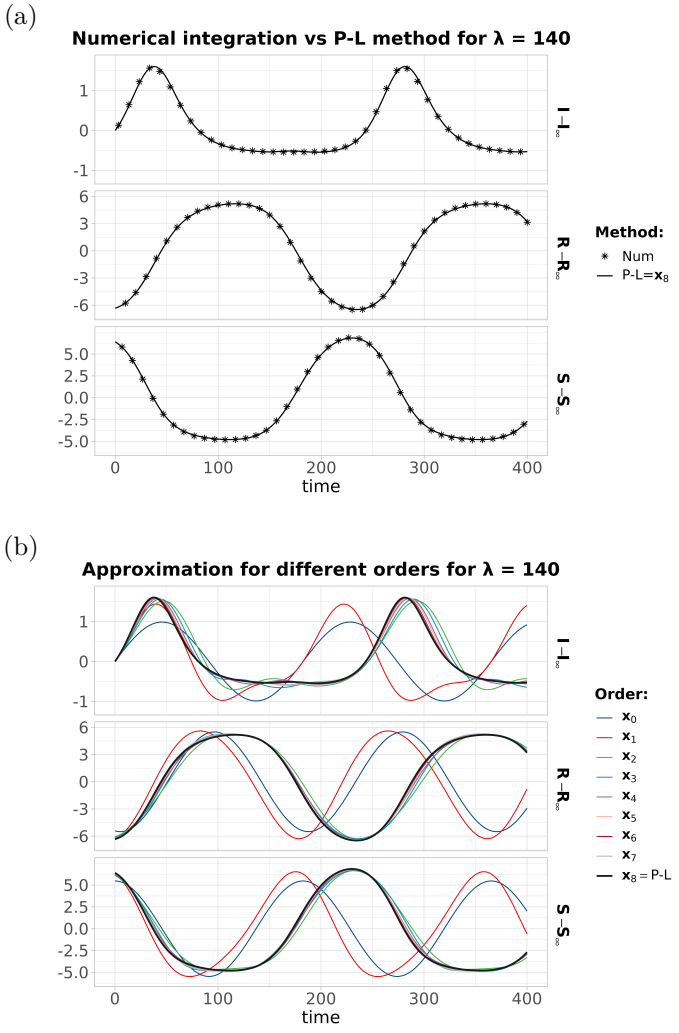

Fig. 4. Asymptotic stable solution of I, R and S for $\lambda = 140$ days in model in eq. (4.6): (a) numerical solution $\tilde{\mathbf{x}}(t_0+t)$ and P-L calculation $\mathbf{x}_8(t)$, (b) approximation for each series expansion order. $\tilde{\varepsilon} = 5.602$

Table 8
Relative errors [%] for the SIR model scenario

	Error [%]	$\mathbf{x}_2$	$\mathbf{x}_3$	$\mathbf{x}_4$	$\mathbf{x}_5$	$\mathbf{x}_6$	$\mathbf{x}_7$	$\mathbf{x}_8$
$\lambda = 120$ days	r_r	10.47	5.17	1.88	1.34	0.62	0.47	0.16
	e_r	16.42	23.28	3.06	5.06	0.72	1.6	0.32
$\lambda = 140$ days	r_r	29.87	16.03	8.51	5.91	4.39	3.11	2.14
	e_r	37.32	74.44	8.63	21.42	3.40	9.57	2.93

These results show the generality of the developed methodology to solve problems in different areas, and the applicability of the method to obtain explicit solutions in complex delayed problems, including DDEs of order greater than 2, or systems of DDEs of higher dimension.

4.3. MACROECONOMIC MODEL

Finally, to further illustrate the practicality of the method, we apply it to a model frequently studied in finance analysis, which relates time series for different macroeconomic variables, namely interest rate, price index and investment demand, to study the formation of monetary cycles.

4.3.1. System of equations and equilibrium solution

We follow the reference [28], where an analysis of the asymptotic stability and the Hopf bifurcation characterization is offered for the following delayed macroeconomic system:

$$\begin{aligned} R'(t) &= (I(t) - \alpha)R(t) + P(t - \lambda), \\ I'(t) &= 1 - \beta I(t) - R(t)^2, \\ P'(t) &= -R(t) - \gamma P(t), \end{aligned} \tag{4.9}$$

where $R(t)$ is the interest rate, $I(t)$ is the investment demand, $P(t)$ is the price index, $\alpha > 0$ is the saving amount, $\beta > 0$ is the cost of the investment and $\gamma > 0$ is the elasticity of demand of commercial markets. In this model it is considered that the price change does not immediately affect the interest rate, for which there is a delay λ. The original reference [28] provides a detailed analysis of the system (4.9), of which the main results follow.

We consider the equilibrium solution when $t \to \infty$ ($R(\infty) = 0$, $I(\infty) = \frac{1}{\beta}$, $P(\infty) = 0$). The linearized system around this equilibrium point is the following:

$$\begin{aligned} R'(t) &= \frac{-\alpha\beta + 1}{\beta} R(t) + P(t - \lambda), \\ I'(t) &= -\beta I(t), \\ P'(t) &= -R(t) - \gamma P(t). \end{aligned} \tag{4.10}$$

This system is characterized by the matrices:

$$\mathbf{P} = \begin{pmatrix} \frac{-\alpha\beta+1}{\beta} & 0 & 0 \\ 0 & -\beta & 0 \\ -1 & 0 & -\gamma \end{pmatrix},$$

$$\mathbf{Q} = \begin{pmatrix} 0 & 0 & 1 \\ 0 & 0 & 0 \\ 0 & 0 & 0 \end{pmatrix}.$$

We again calculate the critical delay λ_0 and the critical periodic solution of period ω_0 corresponding to the Hopf bifurcation by means of the characteristic equation in terms of the complex variable z:

$$(z+\beta)\left(z^2+\left(\alpha+\gamma-\frac{1}{\beta}\right)z+\left(\alpha-\frac{1}{\beta}\right)\gamma+e^{-z\lambda}\right)=0.$$

Apart from the obvious root $z=-\beta$, we search for solutions of the form $z=j\omega_0$ for a given delay λ_0. It can be proved that if the condition $\alpha\beta\gamma-\gamma-\beta<0$ holds, there exist a unique positive solution for ω_0 (see [28]):

$$\omega_0=\sqrt{\frac{-(\alpha-\frac{1}{\beta})^2-\gamma^2+\sqrt{((\alpha-\frac{1}{\beta})^2-\gamma^2)^2+4}}{2}}, \tag{4.11}$$

determined by the delay values:

$$\lambda_0^i=\frac{1}{\omega_0}\Big(\arccos\Big(\omega_0^2-\Big(\alpha-\frac{1}{\beta}\Big)\gamma\Big)+2\pi i\Big).$$

In [28] it is proved that these parameters determine a Hopf bifurcation asymptotically stable. We will be interested in the lowest value for the delay λ_0^i:

$$\lambda_0^0=\lambda_0=\frac{1}{\omega_0}\Big(\arccos\Big(\omega_0^2-\Big(\alpha-\frac{1}{\beta}\Big)\gamma\Big)\Big). \tag{4.12}$$

4.3.2. Explicit expression of periodic solutions

We will consider the parameters for system (4.9) included in Table 9 (as in the original reference we use here dimensionless parameters).

Table 9
Parameters used in the study of the financial model (4.9)

Parameter	Description	Value
α	Savings amount	0.5
β	Cost of investment	0.8
γ	Elasticity of demand	0.8

Under these conditions, the equilibrium point can be calculated using (4.11) and (4.12):

$$\omega_0=0.6321,$$
$$\lambda_0=0.05.$$

Taking these values, we obtain the following orthonormal basis for the solutions of the linearized system (4.10) in the scaled time $\tau = \omega_0 t$:

$$\begin{aligned} \mathbf{v}_1(\tau) &= (0.4028\cos(\tau), 0, -0.3100\cos(\tau) - 0.2450\sin(\tau)), \\ \mathbf{v}_2(\tau) &= (0.4028\sin(\tau), 0, -0.3100\sin(\tau) + 0.2450\cos(\tau)), \end{aligned} \tag{4.13}$$

and the basis for the adjoint system:

$$\begin{aligned} \mathbf{w}_1(\tau) &= (-0.4028\sin(\tau), 0, -0.2546\cos(\tau) - 0.3021\sin(\tau)), \\ \mathbf{w}_2(\tau) &= (0.4028\cos(\tau), 0, -0.2546\sin(\tau) + 0.3021\cos(\tau)). \end{aligned}$$

Notice that in this case the function for the second component of the two bases is 0. This does not mean that the second component of the periodic solution will be null, but rather that it will be composed of terms with frequencies $n\omega_0$ with $n > 1$, as we will see.

We now use these values to derive the approximations to the solutions of $\mathbf{Z}(\tau, \epsilon)$, $\hat{\lambda}(\epsilon)$ and $\hat{T}(\epsilon)$. We recall that he fundamental solution $\mathbf{Z}_0(\tau)$ has to be compatible with the phase condition (2.10), therefore $\mathbf{Z}_0(\tau) = \sqrt{2\pi} \cdot \mathbf{v}_2(\tau)$. Using this as our first solution, we iteratively calculate the subsequent orders following the described methodology. The results for the expansion of the delay and the period are presented (up to order 5) in Table 10. Again, the coefficients for the series expansions for the vector solution are omitted for conciseness.

Table 10
Coefficients for series expansion of λ and T

Coef.	o0	o1	o2	o3	o4	o5
$\hat{\lambda}_i$	0.031608	0	0.34529	0	0.18990	0
$\hat{T}_i$	2π	0	−5.20429	0	5.5555	0

It is worth noting that even when the parameters $\hat{\lambda}_i$ and $\hat{T}_i$ are null, as is the case for order 1, 3 and 5, there are still nonzero terms for those orders for the variable I. Also, the variables R and P have null coefficients for the even trigonometric orders, while variable I has null coefficients for the odd ones. This is why the corresponding component of the fundamental solution of the linearized system (4.13) is null, as has been pointed out before. The results for the approximation obtained with the Poincaré–Lindstedt method compared to the solution calculated by numerical integration are presented below. The numerical integration results are calculated with the initial condition of $r_0 = 0.3$, $I_0 = -0.3$ and $P_0 = 0$, taking the steady state after a sufficiently large initial time, while the explicit calculation by Poincaré–Lindstedt method is directly calculated up to the order 8. Figures 5 (a) and 5 (b) presents the comparison of the solutions of system (4.9) for a delay $\lambda = 0.1$. It can be seen that for this comparably high delay value the approximation is remarkably close to the numerical integration, while it is needed to calculate at least four expansion orders in order to get a suitable approximation.

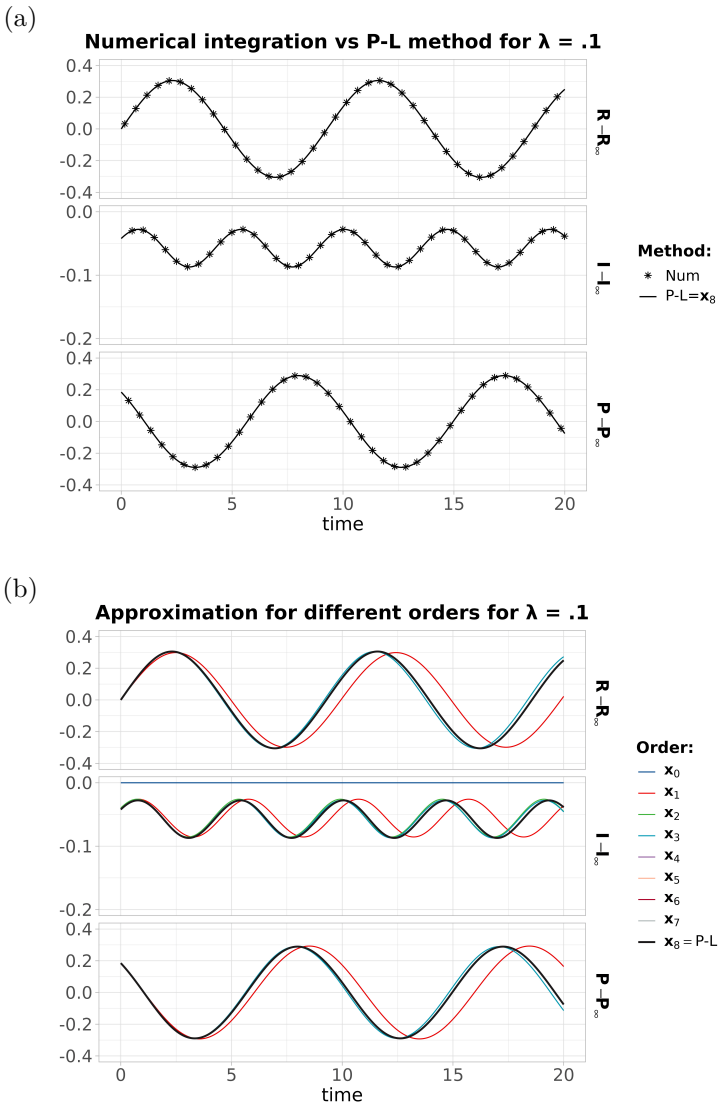

Fig. 5. Asymptotic stable solution of $R(t)$, $I(t)$ and $P(t)$ for $\lambda = 0.1$ in model in eq. (4.9): (a) numerical solution and P-L calculation up to $o8$, (b) approximation for each series expansion order. $\tilde{\varepsilon} = 0.2956$

Notice that, in this particular problem, the base frequency for the investment component I is twice the fundamental frequency of the linear problem ω_0, reflecting the fact that the value for this component in the linear solution basis is 0. Finally, the bifurcation diagram is included in Figure 6 and the relative error in Table 11.

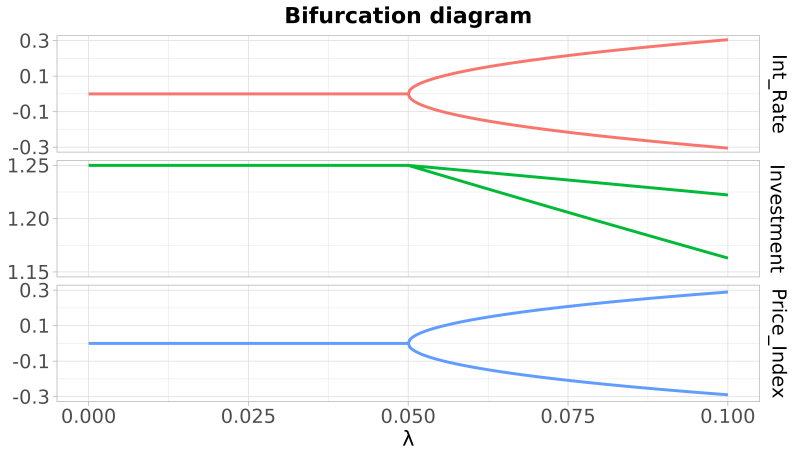

Fig. 6. Bifurcation diagram for the macroeconomic model (4.9)

Table 11
Relative errors [%] for the macroeconomic model scenario

	Error [%]	$\mathbf{x}_2$	$\mathbf{x}_3$	$\mathbf{x}_4$	$\mathbf{x}_5$	$\mathbf{x}_6$	$\mathbf{x}_7$	$\mathbf{x}_8$
$\lambda = 0.08$	r_r	0.54	0.19	0,03	0.01	< 0.01	< 0.01	< 0.01
	e_r	2.17	2.18	0.05	0.05	< 0.01	< 0.01	< 0.01
$\lambda = 0.1$	r_r	1.2	0.52	0.10	0.06	0.01	< 0.01	< 0.01
	e_r	4.74	4.77	0.22	0.21	0.02	< 0.01	< 0.01

5. CONCLUSION

This paper has introduced a complete methodology and technical result for the calculation of precise series expansions for the periodic solutions that stem in the vicinity of the Hopf bifurcations in DDEs. The methodology extends the general methodology provided in [5], allowing the implementation of the iterative calculations using any modern symbolic and numerical computation system, and enabling to carry on the calculations up to the desired order expansion, with the only possible limitation of the numerical precision and memory capacity of the computing platform.

This methodology offers clear advantages over existing numerical integration methods when calculating precise periodic solutions for Hopf bifurcations in DDEs: on the one hand, numerical integration methods require additional checks to ensure that the solution has reached the periodic phase after the initial transient phase, which may be time consuming, specially in systems in which the frequency and amplitude of the solution converge very slowly in time; on the other hand, this method allows for precise calculations of the frequency and amplitude of the steady-state solution instantly, taking advantage of pre-computed coefficients for the series expansions of the solution.

The results presented show remarkable accuracy, with the only requirement of using ever more terms in the series expansion the higher the value of the delay we are studying. It is worth mentioning that in the examples presented we managed to get relative errors below 1% for values of delay 35% greater than the bifurcation value. This can be efficiently managed if the coefficients are pre-computed up to a sufficiently high order. Moreover, this allows the calculation of high precision bifurcation diagrams almost instantly. In our numerical experiments we have managed to calculate the coefficients up to order 20 before we reach the limits of the machine capacity in a standard installation.

It has been also verified that the error management based on the residual of the DDE can provide sufficient accuracy to implement efficient error control schemes that do not depend on the availability of error bounds from numerical integration.

In summary, the method is general enough to be applied to a wide spectrum of problems of considerable complexity for which there were not available procedures for deriving accurate explicit solutions before. Areas of study in which a closed expression for the solution of a DDE is necessary can benefit from the application of this methodology, specially for scenarios far from the bifurcation point. Evolution of this method to bifurcations of higher dimension is intended as future work.

Acknowledgements
The authors would like to thank Prof. Alfonso Casal for his careful reading of the paper and for his insightful comments. The authors were partially supported by the Aula Universidad Empresa of the UPM, BID-Group One on the Quality Culture, and the second author was partially supported by the Spanish Project PID2020-112517GB-I00 of the Ministerio de Ciencia e Innovación (Spain).

REFERENCES

[1] M. Bando, K. Hasebe, A. Nakayama, A. Shibata, Y. Sugiyama, *Dynamical model of traffic congestion and numerical simulation*, Phys. Review E **51** (1995), 1035–1042.

[2] C.M. Batistela, D.P.F. Correa, Á.M. Bueno, J.R.C. Piqueira, *SIRSI compartmental model for COVID-19 pandemic with immunity loss*, Chaos, Solitons and Fractals **142** (2021), 110388.

[3] F. Brauer, C. Castillo-Chavez, *Mathematical Models in Population Biology and Epidemiology*, Springer, New York, 2012.

[4] A. Bridgewater, B. Huard, M. Angelova, *Amplitude and frequency variation in nonlinear glucose dynamics with multiple delays via periodic perturbation*, J. Nonlinear Sci. **30** (2020), 737–766.

[5] A. Casal, M. Freedman, *A Poincaré–Lindstedt approach to bifurcation problems for differential-delay equations*, IEEE Trans. Automat. Control **25** (1980), 967–973.

[6] O. Diekmann, J.A.P. Heesterbeek, J.A.J. Metz, *On the definition and the computation of the basic reproduction ratio R0 in models for infectious diseases in heterogeneous populations*, J. Math. Biol. **28** (1990), 365–382.

[7] P. van den Driessche, J. Watmough, *Reproduction numbers and sub-threshold endemic equilibria for compartmental models of disease transmission*, Math. Biosci. **180** (2002), 29–48.

[8] L.C. Edie, *Car-following and steady-state theory for noncongested traffic*, Oper. Res. **9** (1961), 66–76.

[9] N.B. Ferguson, B.A. Finlayson, *Error bounds for approximate solutions to nonlinear ordinary differential equations*, AIChE Journal **18** (1972), 1053–1059.

[10] D.C. Gazis, R. Herman, R.B. Potts, *Car-following theory of steady-state traffic flow*, Oper. Res. **7** (1959), 499–505.

[11] D.C. Gazis, R. Herman, R.W. Rothery, *Nonlinear follow-the-leader models of traffic flow*, Oper. Res. **9** (1961), 545–567.

[12] D.E. Gilsinn, *On algorithms for estimating computable error bounds for approximate periodic solutions of an autonomous delay differential equation*, Commun. Nonlinear Sci. Numer. Simul. **14** (2009),1526–1550.

[13] Z. Guo, X. Ma, *Residue harmonic balance solution procedure to nonlinear delay differential systems*, Appl. Math. Comput. **237** (2014), 20–30.

[14] J.K. Hale, *Theory of Functional Differential Equations*, Springer-Verlag, New York, 1977.

[15] H.W. Hethcote, *The mathematics of infectious diseases*, SIAM Rev. **42** (2000), 599–653.

[16] Z. Lv, J. Zeng, Y. Ding, X. Liu, *Stability analysis of time-delayed SAIR model for duration of vaccine in the context of temporary immunity for COVID-19 situation*, Electron. Res. Arch. **31** (2023), 1004–1030.

[17] A.H. Nayfeh, D.T. Mook, *Nonlinear Oscillations*, John Wiley & Sons, 2008.

[18] G.F. Newell, *Nonlinear effects in the dynamics of car following*, Oper. Res. **9** (1961), 209–229.

[19] J.F. Padial, A. Casal, *Bifurcation in car-following models with time delays and driver and mechanic sensitivities*, Rev. R. Acad. Cienc. Exactas Fis. Nat. **116** (2022), 180.

[20] B. Pell, M.D. Johnston, P. Nelson, *A data-validated temporary immunity model of COVID-19 spread in Michigan*, Math. Biosci. Eng. **19** (2022), 10122–10142.

[21] R. Rand, *Differential-delay equations*, [in:] A.C.J. Luo, J.Q. Sun (eds.), *Complex Systems: Fractionality, Time-delay and Synchronization*, Springer Science and Business Media, 2011.

[22] M.Q. Shakhany, K. Salimifard, *Predicting the dynamical behavior of COVID-19 epidemic and the effect of control strategies*, Chaos, Solitons and Fractals **146** (2021), 110823.

[23] B. Shayak, M.M. Sharma, M. Gaur, A.K. Mishra, *Impact of reproduction number on the multiwave spreading dynamics of COVID-19 with temporary immunity: A mathematical model*, Int. J. Infec. Dis. **104** (2021), 649–654.

[24] H.L. Smith, *An Introduction to Delay Differential Equations with Applications to the Life Sciences*, Springer, New York, 2011.

[25] F. Verhulst, *Nonlinear Differential Equations and Dynamical Systems*, Springer, Berlin, 1996.

[26] M. Xiao, J. Cao, *Approximate expressions of the bifurcating periodic solutions in a neuron model with delay-dependent parameters by perturbation approach*, Cogn. Neurodyn. **4** (2010), 241–250.

[27] M. Xiao, G. Jiang, L. Zhao, W. Xu, Y. Wan, C. Fan, Z. Wang, *Stability switches and Hopf bifurcations of an isolated population model with delay-dependent parameters*, Appl. Math. Comput. **264** (2015), 99–115.

[28] X. Zhang, H. Zhu, *Hopf bifurcation and chaos of a delayed finance system*, Complexity **2019** (2019), 6715036.

José Enríquez Gabeiras (corresponding author)
jose.enriquez@alumnos.upm.es
https://orcid.org/0009-0002-0496-1282

Universidad Politécnica de Madrid
Department of Applied Mathematics
Madrid, Spain

Juan Francisco Padial Molina
jfpadial@upm.es
https://orcid.org/0000-0001-7092-3554

Universidad Politécnica de Madrid
Department of Applied Mathematics
Madrid, Spain

Received: February 16, 2025.
Revised: April 2, 2025.
Accepted: April 5, 2025.